



OPEN

Retinal ganglion cell analysis in patients with sellar and suprasellar tumors with sagittal bending of the optic nerve

Yoichiro Shinohara^{1✉}, Daisuke Todokoro¹, Rei Yamaguchi², Masahiko Tosaka², Yuhei Yoshimoto² & Hideo Akiyama¹

The study investigated clinical features of sellar and suprasellar tumors with optic nerve bending. Twenty-five patients (13 men/12 women; age, 59.0 ± 12.9 years) with optic nerve bending in one eye who underwent tumor resection for sellar and suprasellar tumors were included. The other eye, without optic nerve bending, was the control. The pre- and postoperative best-corrected visual acuity (BCVA) and ganglion cell layer (GCL) + inner plexiform layer (IPL) thickness were studied retrospectively using optical coherence tomography. Preoperative BCVA in the eye with optic nerve bending was significantly poor and improved significantly after tumor resection. Eyes with optic nerve bending had significantly less GCL + IPL thickness on the temporal side than eyes without optic nerve bending. Preoperative GCL + IPL thickness of the entire macula was reduced in eyes with optic nerve bending and poor postoperative BCVA compared to those with good postoperative BCVA. There was no significant difference in GCL + IPL thickness of eyes with optic nerve bending before and after tumor resection. Optic nerve bending caused by sellar and suprasellar tumors resulted in visual impairment and decreased retinal ganglion cells. Eyes with optic nerve bending and severely reduced GCL + IPL thickness may have less BCVA improvement after tumor resection.

Sellar and suprasellar tumors, including pituitary adenomas, show visual field defects, such as bilateral hemianopsia, due to the optic chiasm compression by the tumor¹. Visual field impairment progresses gradually as the tumor grows, resulting in visual impairment^{2,3}. However, even a relatively slight compression of the optic chiasm can cause visual impairment. We investigated the visual acuity impairment in the patients with sellar and suprasellar lesions using magnetic resonance (MR) T2 weighted imaging⁴. We also reported a new concept that the optic nerve sometimes bends at the entrance of the optic canal from the intracranial subarachnoid space. Further, a combination of preoperative optic nerve bending and optic chiasm compression is associated with visual impairment (Fig. 1)⁴. The effect of optic nerve bending caused by sellar and suprasellar tumors on the retina remains unclear. Optical coherence tomography (OCT) can measure ganglion cell layer (GCL) + inner plexiform layer (IPL) thickness in the macula with high reliability. Previous reports showed the usefulness of macular GCL + IPL parameters in discriminating early glaucoma from normal eyes⁵. Morphological changes in retinal ganglion cells might also be observed using OCT in patients with sellar and suprasellar tumors with optic nerve bending. Here, we investigated the OCT findings of patients with sellar and suprasellar tumors with optic nerve bending before and after tumor resection.

Results

Demographic characteristics and visual acuity. Table 1 shows patients' demographic and clinical characteristics with sellar and suprasellar tumors. Regarding the sellar and suprasellar tumors, 15, 4, 3, and 3 patients had pituitary adenoma, craniopharyngioma, Rathke's cleft cyst, and meningioma, respectively. Patients

¹Department of Ophthalmology, Gunma University Graduate School of Medicine, 3-39-15 Showa machi, Maebashi, Gunma 371-8511, Japan. ²Department of Neurosurgery, Gunma University Graduate School of Medicine, Maebashi, Gunma, Japan. ✉email: shinohara@gunma-u.ac.jp

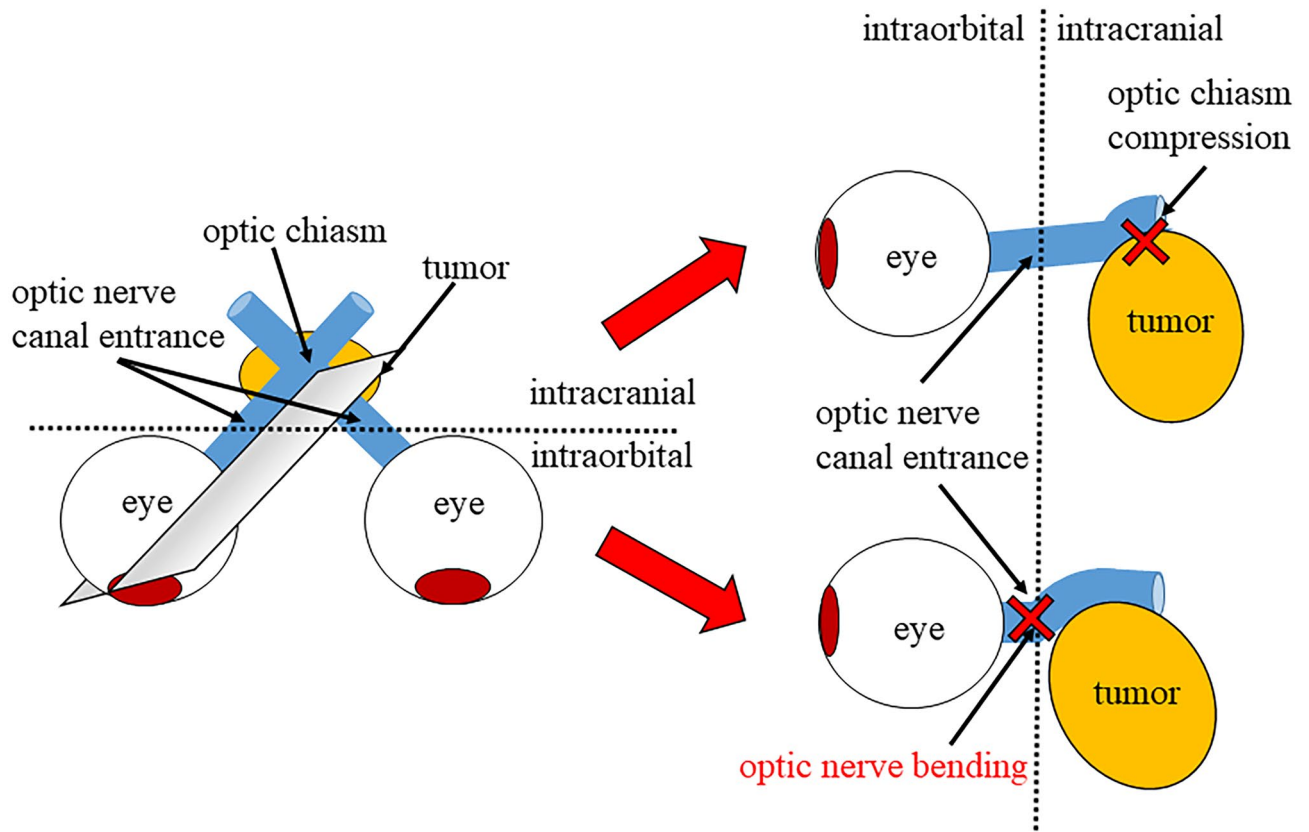


Figure 1. Schema from the eyeball to the optic chiasm in a patient with sellar and suprasellar tumor. The gray polygon in the left panel showed a cross-section of the path from the eyeball to the optic chiasm, as shown in the right panel. The upper right panel showed a schema of optic chiasm compression by the suprasellar and suprasellar tumor. The lower right panel showed a schema of optic nerve bending by the suprasellar and suprasellar tumor. The enlarged sellar and suprasellar tumor causes visual field defects due to optic chiasm compression. However, sellar and suprasellar tumors, with or without optic chiasm compression, sometimes bend the optic nerve at the optic canal’s entrance, leading to visual impairment.

	Subject (n = 25)	
	Optic nerve bending (+)	Optic nerve bending (-)
Number of eyes (n)	25	25
Age (years)	59.0 ± 12.9	
Male:female (n)	13:12	
Pathology (n)		
Pituitary adenoma	15	
Craniopharyngioma	4	
Rathke’s cleft cyst	3	
Meningioma	3	
Right eye (n)	14	11
Left eye (n)	11	14
ONCBA (°)	56.7 ± 11.0	27.2 ± 8.4

Table 1. Systemic characteristics of patients with sellar and suprasellar tumors. ONCBA optic nerve–canal bending angle.

with the sellar and suprasellar tumors included 13 men (52.0%) and 12 women (48.0%). Their average age was 59.0 ± 12.9 years. The mean optic nerve–canal bending angles (ONCBAs) were 56.7 ± 11.0° in bending eyes and 27.2 ± 8.4° in non-bending eyes (p < 0.001). Tables 2 and 3 show ONCBA and ophthalmologic parameters of all patients. Preoperative and postoperative best-corrected visual acuities (BCVAs) (logMAR) were 0.27 ± 0.33 and -0.03 ± 0.12 and 0.03 ± 0.23 and -0.06 ± 0.05 in bending and non-bending eyes, respectively (Fig. 2a). Preoperative BCVA of the bending eyes was significantly lower than that of the non-bending eyes (p < 0.001). Post-

No.	ONCBA	Pre-op							Post-op						
		GCIPL (μm)							GCIPL (μm)						
		BCVA	S	SN	IN	I	IT	ST	BCVA	S	SN	IN	I	IT	ST
1	46	0.15	65	63	62	67	73	72	0.05	66	63	61	66	73	72
2	76	1.00	67	67	65	67	73	69	-0.08	63	62	60	63	71	66
3	54	0.00	78	77	69	70	80	79	-0.08	78	76	69	69	78	79
4	76	0.82	63	64	65	69	75	69	-0.08	62	62	62	67	74	66
5	59	0.22	79	82	77	76	85	82	-0.08	79	82	74	74	84	81
6	99	0.10	61	61	56	55	59	56	0.05	62	61	56	56	58	58
7	48	0.05	84	83	80	80	83	83	-0.08	85	83	79	78	82	81
8	72	0.52	60	59	56	58	73	65	-0.08	62	60	55	59	70	65
9	45	0.22	67	67	65	70	78	73	0.00	65	65	62	73	79	73
10	70	0.05	67	64	61	70	79	73	-0.08	66	63	61	68	79	72
11	53	0.22	83	87	84	78	78	79	-0.08	82	86	82	74	75	76
12	84	0.10	62	54	55	66	83	78	-0.08	61	53	54	64	82	77
13	73	0.82	48	51	48	54	63	53	0.70	49	49	47	53	60	50
14	47	-0.08	74	68	64	72	84	83	-0.08	75	68	63	71	83	82
15	55	1.05	23	30	27	23	23	26	0.70	24	23	24	21	23	22
16	71	-0.08	59	59	57	64	78	68	-0.08	56	56	53	62	75	66
17	76	-0.08	77	79	75	74	81	77	-0.08	78	79	75	75	83	79
18	45	-0.08	60	46	44	59	74	72	-0.08	61	47	46	60	75	73
19	49	0.52	73	72	71	75	80	75	-0.08	73	72	71	75	80	75
20	62	-0.08	71	79	73	65	63	67	-0.08	66	74	76	71	62	67
21	69	0.30	68	64	58	63	75	73	0.40	66	63	58	64	75	71
22	47	0.30	79	74	70	74	83	78	-0.08	80	75	70	75	83	79
23	45	0.15	57	53	52	62	77	71	0.15	56	53	51	59	75	72
24	48	0.22	48	46	46	51	57	58	0.15	49	46	45	51	57	58
25	61	0.30	68	70	68	34	65	68	-0.08	67	68	65	67	71	68

Table 2. Angle of bending and ophthalmologic parameters of patients with optic nerve bending. ONCBA optic nerve–canal bending angle, BCVA best-corrected visual acuity(logMAR).

operative BCVA was significantly better than preoperative BCVA in the bending eyes ($p < 0.01$) (Fig. 2a). No significant differences were found between the preoperative and postoperative BCVA in non-bending eyes. In addition, Spearman's correlation ($r = 0.4986$, $p = 0.0002$) shows that ONCBA was positively correlated with preoperative BCVA in 50 eyes of 25 patients (Fig. 2b). Postoperative BCVA and GCL + IPL thickness in all sectors did not correlate with ONCBA.

All 25 patients with optic nerve bending were classified by age into groups of 30–40 s ($n = 6$), 50 s ($n = 7$), 60 s ($n = 5$), and 70 s ($n = 7$). Postoperative BCVAs (logMAR) were -0.08 ± 0.00 (30–40 s), 0.01 ± 0.17 (50 s), 0.08 ± 0.31 (60 s) and 0.13 ± 0.25 (70 s), respectively. Postoperative BCVA showed no significant differences among these 4 groups (all $p > 0.05$, a one-way analysis of variance followed by Tukey's post hoc test).

Assessment of GCL + IPL using OCT. The preoperative GCL + IPL thicknesses in bending and non-bending eyes were $65.6 \pm 12.8 \mu\text{m}$ and $71.4 \pm 9.7 \mu\text{m}$ in the superior sector, $64.8 \pm 13.1 \mu\text{m}$ and $68.8 \pm 11.1 \mu\text{m}$ in the superior nasal sector, $61.9 \pm 12.4 \mu\text{m}$ and $64.8 \pm 10.6 \mu\text{m}$ in the inferior nasal sector, $63.8 \pm 12.9 \mu\text{m}$ and $70.0 \pm 8.4 \mu\text{m}$ in the inferior sector, $72.9 \pm 12.8 \mu\text{m}$ and $80.6 \pm 11.5 \mu\text{m}$ in the inferior temporal sector, and $69.9 \pm 11.8 \mu\text{m}$ and $75.8 \pm 8.0 \mu\text{m}$ in the superior temporal sector, respectively. The postoperative GCL + IPL thicknesses in the bending and non-bending eyes were $65.2 \pm 12.7 \mu\text{m}$ and $71.0 \pm 9.1 \mu\text{m}$ in the superior sector, $63.6 \pm 13.7 \mu\text{m}$ and $68.2 \pm 10.7 \mu\text{m}$ in the superior nasal sector, $60.8 \pm 12.6 \mu\text{m}$ and $64.6 \pm 10.5 \mu\text{m}$ in the inferior nasal sector, $64.6 \pm 11.4 \mu\text{m}$ and $68.4 \pm 8.2 \mu\text{m}$ in the inferior sector, $72.3 \pm 12.7 \mu\text{m}$ and $79.9 \pm 12.3 \mu\text{m}$ in the inferior temporal sector, and $69.1 \pm 12.4 \mu\text{m}$ and $75.6 \pm 8.0 \mu\text{m}$ in the superior temporal sector, respectively (Fig. 3a–f). There was no significant difference in GCL + IPL thickness before and after surgery in all sectors (all $p > 0.05$). In both bending and non-bending eyes, the GCL + IPL thickness was lesser in the nasal sectors than in the temporal sectors, both before and after surgery. Notably, the GCL + IPL thickness in the superior temporal and inferior temporal sectors was significantly lesser in the bending eyes than in the non-bending eyes, both before and after surgery ($p < 0.05$) (Fig. 3e,f).

In bending eyes, we defined 19 eyes with postoperative BCVA (logMAR) of 0 or better as good visual outcome and 6 eyes with postoperative BCVA (logMAR) of less than 0 as poor visual outcome. The preoperative GCL + IPL thicknesses in the good visual outcome eyes and the poor visual outcome eyes were $69.9 \pm 8.1 \mu\text{m}$ and $52.0 \pm 15.3 \mu\text{m}$ in the superior sector, $68.7 \pm 10.5 \mu\text{m}$ and $52.3 \pm 12.8 \mu\text{m}$ in the superior nasal sector, $65.7 \pm 9.6 \mu\text{m}$ and $49.8 \pm 12.5 \mu\text{m}$ in the inferior nasal sector, $68.9 \pm 6.6 \mu\text{m}$ and $47.8 \pm 14.6 \mu\text{m}$ in the inferior sector, $76.9 \pm 6.7 \mu\text{m}$ and $60.0 \pm 17.9 \mu\text{m}$ in the inferior temporal sector, and $73.6 \pm 6.7 \mu\text{m}$ and $58.2 \pm 16.0 \mu\text{m}$ in

No.	ONCBA	Pre-op							Post-op						
		GCIPL(μm)							GCIPL(μm)						
		BCVA	S	SN	IN	I	IT	ST	BCVA	S	SN	IN	I	IT	ST
1	32	0.10	72	69	60	64	77	75	0.10	66	68	60	68	74	70
2	23	-0.08	66	64	62	67	75	67	-0.08	65	62	57	66	76	67
3	34	-0.08	79	81	77	74	82	78	-0.08	79	79	74	73	80	82
4	31	-0.08	73	70	68	72	76	80	-0.08	73	70	67	71	76	78
5	22	-0.08	77	77	72	75	87	80	-0.08	79	76	78	73	84	83
6	2	0.00	66	59	53	59	68	68	0.00	66	61	54	57	69	68
7	33	-0.08	86	83	79	85	92	89	-0.08	86	83	79	83	91	88
8	39	-0.08	58	54	51	56	70	68	-0.08	59	54	52	56	68	68
9	19	0.05	74	68	61	63	73	74	-0.08	72	68	63	65	75	72
10	21	-0.08	72	58	58	79	91	88	-0.08	73	57	57	78	90	87
11	19	-0.08	87	88	81	82	88	81	-0.08	83	85	79	81	88	80
12	24	0.00	66	62	58	71	85	78	-0.08	64	61	57	68	83	78
13	39	-0.08	60	53	50	57	68	70	-0.08	62	53	51	56	67	70
14	30	-0.08	79	73	70	70	80	82	-0.08	78	72	70	72	79	80
15	38	-0.08	66	61	57	63	71	69	-0.08	65	61	56	62	70	68
16	37	-0.08	79	73	68	77	85	83	0.05	77	70	64	75	82	80
17	42	-0.08	81	83	79	79	79	77	-0.08	81	82	81	80	80	77
18	18	-0.08	51	47	46	59	72	59	-0.08	52	47	46	59	72	62
19	26	-0.08	70	69	64	75	84	76	-0.08	70	69	64	75	84	76
20	16	-0.08	70	77	77	75	77	72	-0.08	71	78	76	71	75	72
21	42	-0.08	71	68	64	72	125	85	-0.08	71	66	64	71	130	86
22	35	-0.08	83	77	71	75	84	83	-0.08	82	77	71	74	82	83
23	13	0.52	50	50	48	57	69	58	0.10	52	50	49	55	66	57
24	24	0.00	67	71	65	65	74	71	-0.08	68	70	65	65	74	72
25	37	-0.08	82	85	82	80	82	84	-0.08	82	85	81	80	83	85

Table 3. Angle of bending and ophthalmologic parameters of patients without optic nerve bending. ONCBA optic nerve–canal bending angle, BCVA best-corrected visual acuity(logMAR).

the superior temporal sector, respectively (Fig. 4). The preoperative GCL + IPL thickness in eyes with poor visual outcome was significantly lesser than that in eyes with good visual outcomes in all sectors ($p < 0.001$, inferior sector; $p < 0.01$, other 5 sectors). Representative images of a patient with pituitary adenoma with optic nerve bending with good and poor visual outcomes are shown in Figs. 5 and 6.

Discussion

We retrospectively investigated the clinical features, including retinal ganglion cells (RGCs) analysis, of sellar and suprasellar tumors with sagittal bending of the optic nerve and compared them with those of non-bending optic nerve controls. Eyes with optic nerve bending due to sellar and suprasellar tumors had worse visual acuity and reduced GCL + IPL thickness in the temporal sectors, as measured by OCT, than eyes without optic nerve bending. In addition, eyes with optic nerve bending showed rapid improvement in visual acuity after tumor resection. Furthermore, in six eyes with poor visual outcome, the preoperative GCL + IPL thickness was significantly lesser than that in 19 eyes with good visual outcome.

Yamaguchi et al. measured the sagittal angle of the optic nerve at the entrance of the optic canal using MR imaging in patients with sellar and suprasellar tumors and reported a new concept that sellar and suprasellar tumors cause not only optic chiasm compression but also optic nerve bending, resulting in visual impairment⁴. ONCBA basically affects ipsilateral vision⁴. Moreover, ipsilateral ONCBA is anatomically unrelated to contralateral visual dysfunction. However, when the ONCBA is large, the tumor is often large; therefore, the visual field defect due to chiasma compression may occur bilaterally. In addition, if the tumor is larger, the ONCBA on the contralateral side may be large. In this study, eyes with optic nerve bending had preoperative visual impairment, whereas eyes without optic nerve bending had good preoperative visual acuity (Fig. 2a). The mechanism of visual impairment due to optic nerve bending caused by sellar and suprasellar tumors remains unknown. The optic nerve at the entrance of the optic canal receives blood flow mainly from the superior pituitary artery, with little blood flow from the ophthalmic artery, which is prone to ischemia. The optic chiasm is rich in blood flow, supplied by branches from the internal carotid artery, anterior cerebral artery, and anterior communicating artery^{6,7}. Hence, the optic nerve bending may be more likely to cause visual impairment due to ischemia than optic chiasm compression because the optic nerve at the optic canal's entrance has less blood flow than the optic chiasm.

The nasal GCL + IPL thickness is reduced in pituitary adenomas compared to normal subjects because tumor-induced optic chiasm compression damages the crossed fibers and retrogradely damages retinal ganglion cells⁸. In the current study, the GCL + IPL thickness was also lesser in the nasal sectors of sellar and suprasellar tumors

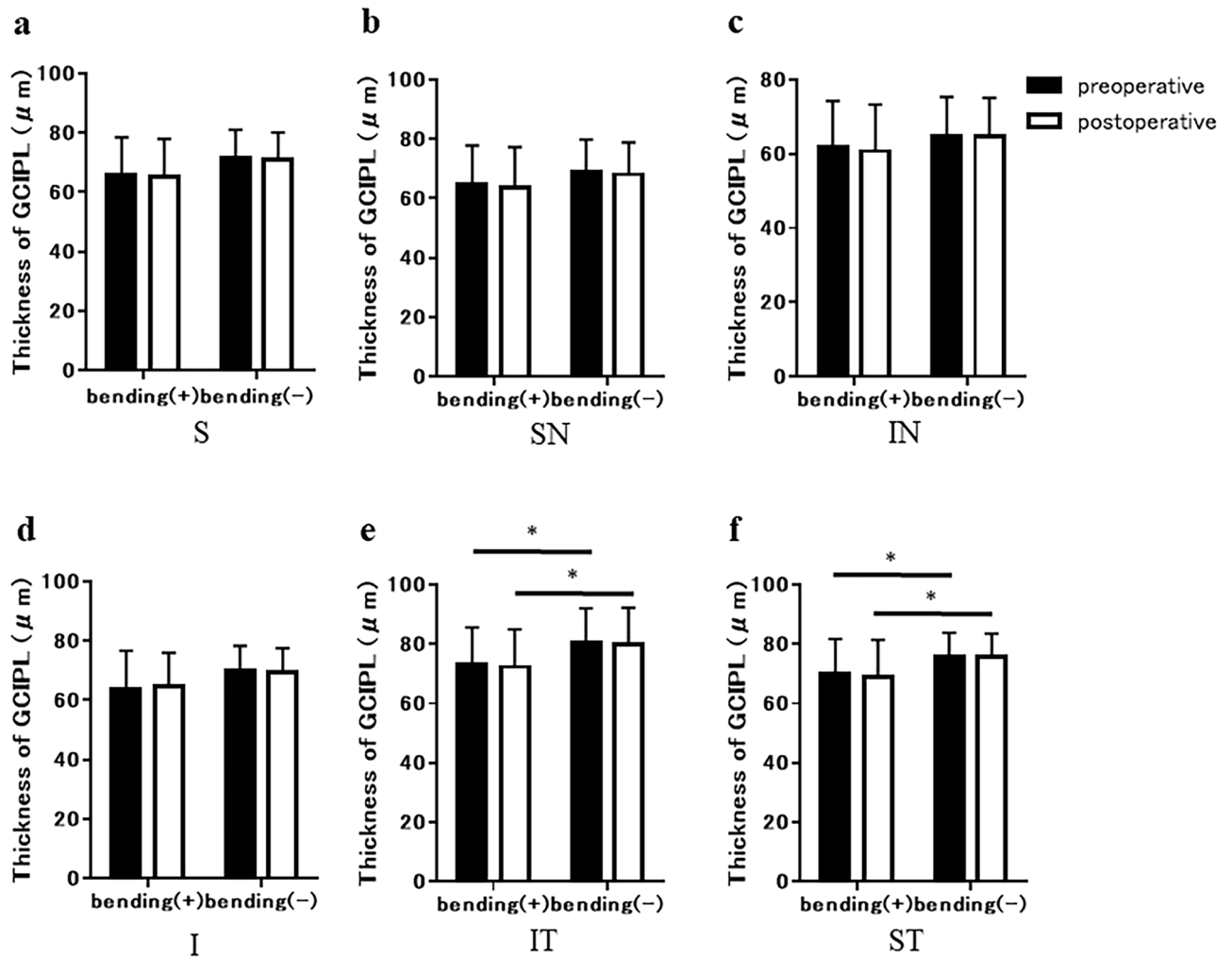


Figure 3. Comparison of ganglion cell layer (GCL) + inner plexiform layer (IPL) thickness between preoperatively (black bar) and postoperatively (white bar) in eyes with and without optic nerve bending. Graphs showed the superior (S) (a), superior nasal (SN) (b), inferior nasal (IN) (c), inferior (I) (d), inferior temporal (IT) (e), and superior temporal (ST) (f) sectors of the macular, respectively. There was no significant difference in pre- and postoperative GCL + IPL thickness in all sectors (all $p > 0.05$). Both preoperatively and postoperatively, GCL + IPL thickness in the inferior temporal (IT) and superior temporal (ST) sectors was significantly lesser in eyes with optic nerve bending than in eyes without optic nerve bending (both $*p < 0.05$).

Methods

Subjects and measurement of clinical examinations. All experiments followed the tenets of the Declaration of Helsinki and were approved by the Institutional Review Board of the Gunma University Graduate School of Medicine (HS2021-097). Informed consent was obtained from all individual participants in the present study. We retrospectively studied 25 patients with visual impairment due to sellar and suprasellar tumors who underwent endoscopic transsphenoidal tumor resection at Gunma University Hospital from June 2015 to July 2021 and had optic nerve bending in only one eye. The other eye, without optic nerve bending, was used as the control. MR imaging of the sellar and suprasellar lesions in all 25 patients with a 1.5 T or 3 T MR imaging system was performed. The presence of optic nerve bending was determined by measuring the sagittal ONCBA

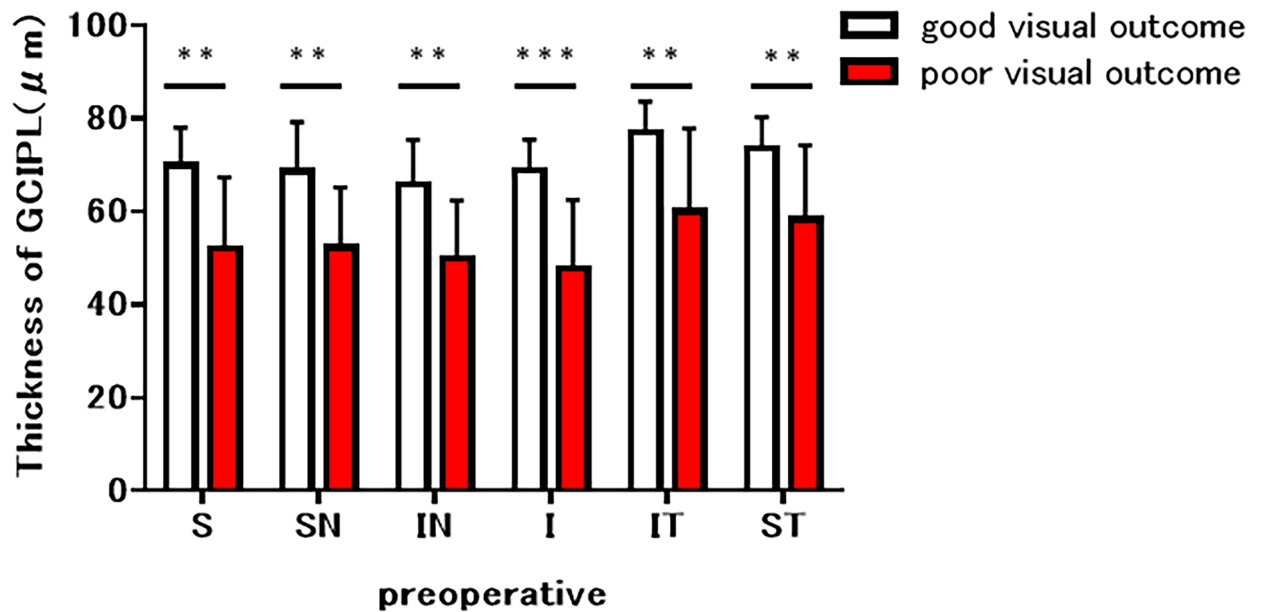


Figure 4. Comparison of preoperative ganglion cell layer (GCL) + inner plexiform layer (IPL) thickness between eyes with and without postoperative visual disturbance in eyes with optic nerve bending. Graphs showed the superior (S), superior nasal (SN), inferior nasal (IN), inferior (I), inferior temporal (IT), and superior temporal (ST) sectors of the macula, respectively. Preoperative GCL + IPL thickness was lesser in eyes with postoperative visual disturbance than in eyes with postoperative non-visual disturbance in all sectors (** $p < 0.001$, inferior sector; ** $p < 0.01$, other 5 sectors).

on MR images before tumor resection, as previously reported⁴. Briefly, the ONCBA is the angle obtained by neurosurgeons measuring the extent of this bending on sagittal MR images formed by the optic nerve in the optic canal and the optic nerve in the intracranial subarachnoid space at the entrance of the optic canal. Each neurosurgeon specializing in pituitary tumor MR reading and surgery (R.Y. and M.T.) made evaluations, and any disagreements regarding conclusions were resolved by consensus. Optic nerve bending (large ONCBA) was defined as ONCBA $\geq 45^\circ$, and non-optic nerve bending (moderate ONCBA) was defined as ONCBA $< 45^\circ$, as previously reported⁴. The exclusion criteria were as follows: (1) patients with a history of glaucoma or evident glaucomatous optic neuropathy; (2) high myopia (refractive error less than -6 diopters); (3) retinal diseases, including epiretinal membrane and macular edema; (4) severe cataract, and (5) unclear optic nerve on MR imaging.

All patients underwent ophthalmologic examinations, including best-corrected visual acuity (BCVA), intraocular pressure assessment, refraction, slit-lamp biomicroscopy, fundus examination, and GCL + IPL thickness measurement, using Cirrus high definition-OCT (Carl Zeiss Meditec, Dublin, CA, USA) in both the optic nerve bending and non-bending eyes before and 1 month after tumor resection (Fig. 7). BCVA was recorded as the decimal visual acuity and converted to logarithm of the minimum angle of resolution (logMAR) notation. The Cirrus HD-OCT ganglion cell analysis (GCA) algorithm automatically segmented the macula into superior, superior nasal, inferior nasal, inferior, inferior temporal, and superior temporal sectors, and measured the GCL + IPL thickness⁵.

Statistical analyses. Data are presented as the mean \pm standard deviation. An unpaired t-test was conducted to compare BCVA and GCL + IPL thickness measurements between the bending and non-bending eyes. The paired t-test was conducted to compare changes in BCVA and GCL + IPL thickness before and 1 month after surgery. The correlation between BCVA and ONCBA was examined using Spearman's correlation coefficient. Statistical significance was set at $p < 0.05$. Statistical analyses were performed using GraphPad Prism version 6 (GraphPad Software Inc., La Jolla, CA, USA).

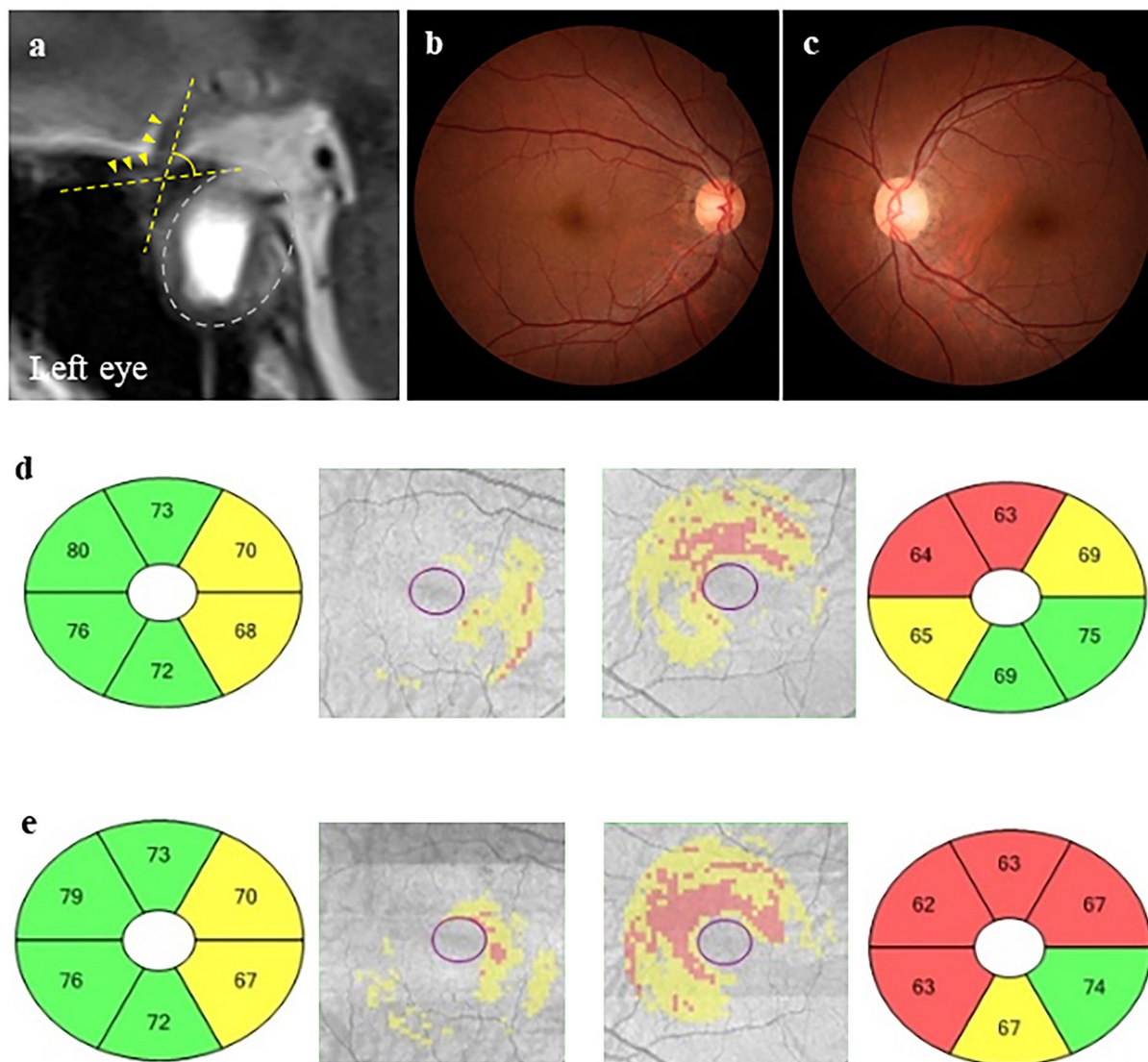


Figure 5. Representative clinical findings of a case with good visual outcome (case 1). A 63-year-old woman with pituitary adenoma with optic nerve bending in the left eye. Preoperative and postoperative best-corrected visual acuities (BCVAs) were -0.08 and -0.08 in the right eye and 0.82 and -0.08 in the left eye logarithm of the minimum angle of resolution units, respectively. **(a)** Preoperative sagittal T2-weighted magnetic resonance images. The optic nerve–canal bending angle (ONCBA) was formed by the optic nerve (nerve indicated by yellow arrowheads) in the optic canal and the optic nerve in the intracranial subarachnoid space at the optic canal’s exit (angle indicated by yellow dotted lines). White dotted lines indicate a tumor. The ONCBAs of this case were 31° in the right eye and 76° in the left eye. Therefore, the left eye is the one with optic nerve bending. **(b, c)** Color fundus photograph showing the normal appearance at preoperative visit (B, right eye; C, left eye). **(d, e)** Ganglion cell layer (GCL) + inner plexiform layer (IPL) deviation map showing the expansion from the parafovea to the periphery of the red area indicates the decrease of GCL + IPL thickness and outside normal limits. GCL + IPL deviation map and sector graph of the right eye (left 2 panels) and left eye (right 2 panels) show a decrease in the macular GCL + IPL thickness, especially from nasal to superior sectors in the left eye. A slight decrease in postoperative GCL + IPL thickness is observed in the left eye (**d**, preoperative; **e**, postoperative visit).

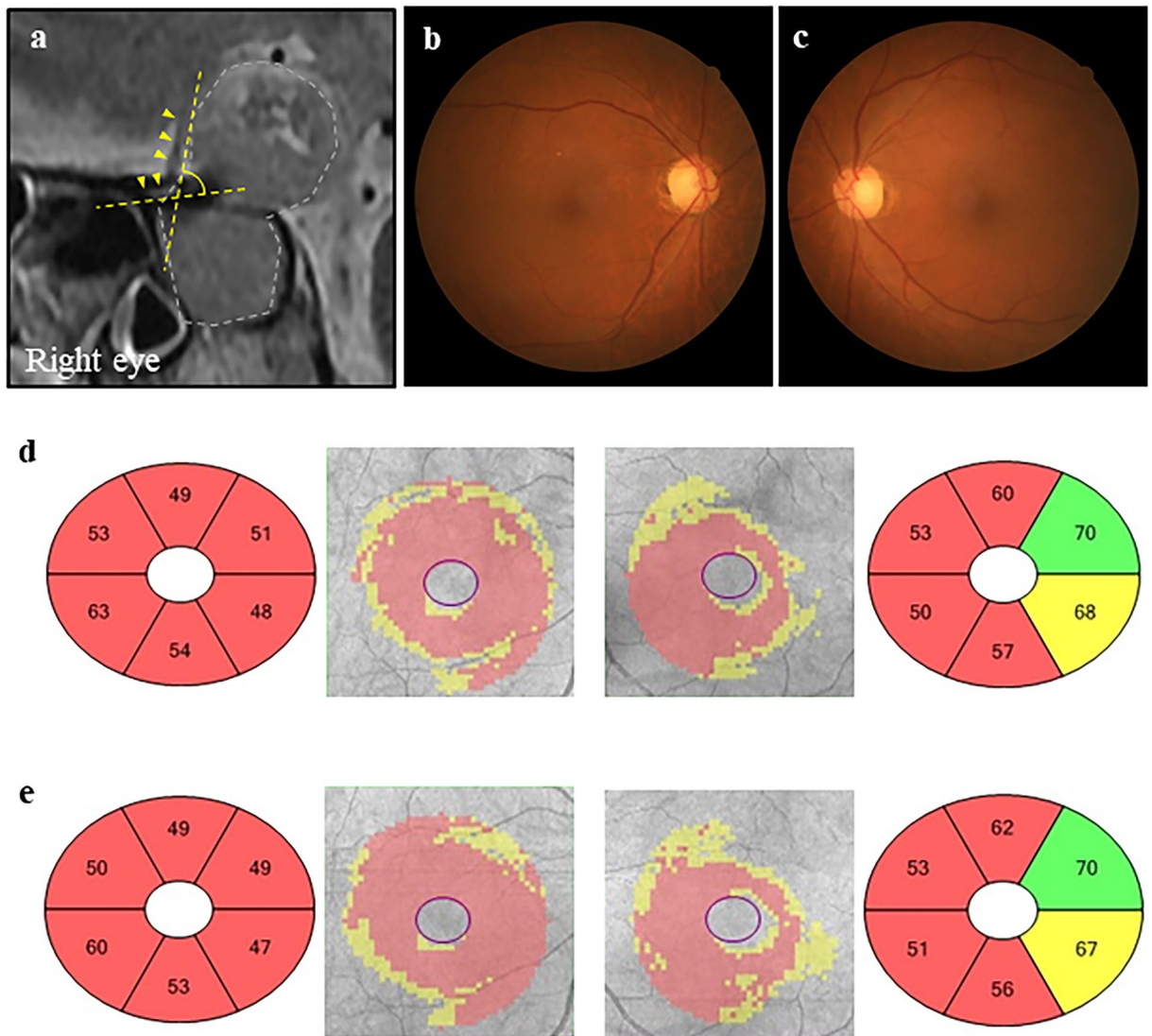


Figure 6. Representative clinical findings of a case with poor visual outcome (case 2). A 74-year-old man with pituitary adenoma with optic nerve bending in the right eye. The preoperative and postoperative best-corrected visual acuities (BCVAs) were 0.82 and 0.10 in the right eye and 0.70 and -0.08 in the left eye logarithm of the minimum angle of resolution units, respectively. **(a)** Preoperative sagittal T2-weighted magnetic resonance images. The angle indicated by yellow dotted lines is the optic nerve–canal bending angle (ONCBA); yellow arrowheads indicate optic nerve, and white dotted lines indicate a tumor. The ONCBAs of this case were 73° in the right eye and 39° in the left eye. Therefore, the right eye is the one with optic nerve bending. **(b, c)** Color fundus photograph showed normal appearance at preoperative visit (B, right eye; C, left eye). **(d, e)** Ganglion cell layer (GCL) + inner plexiform layer (IPL) deviation map and sector graph of the right eye (left 2 panels) and left eye (right 2 panels) (**d**, preoperative; **e**, postoperative visit). A decrease in preoperative GCL + IPL thickness of the right eye is observed in all sectors. A decrease in preoperative GCL + IPL thickness of the left eye is observed in the predominantly nasal region. Postoperative GCL + IPL thickness in almost all sectors was more unremarkable than preoperative GCL + IPL thickness in both eyes.

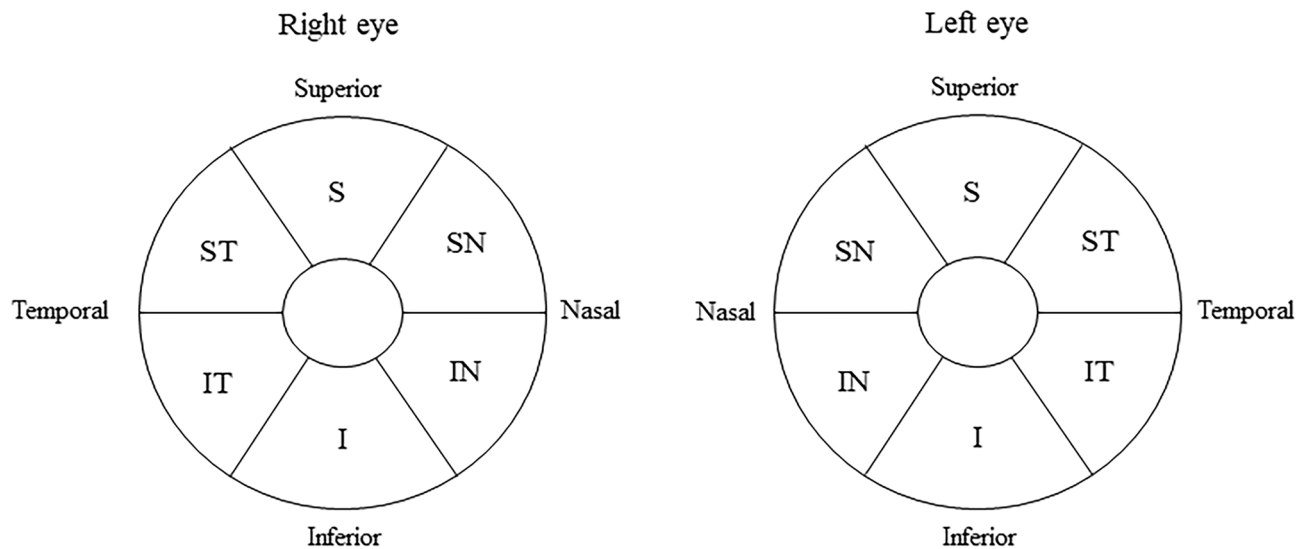


Figure 7. Ganglion cell layer + inner plexiform layer sector map of both eyes using optical coherence tomography. The macular region was divided into six sectors: superior (S), superior nasal (SN), inferior nasal (IN), inferior (I), inferior temporal (IT), and superior temporal sectors (ST).

Data availability

All data generated or analyzed during this study are included in this published article.

Received: 29 January 2022; Accepted: 23 June 2022

Published online: 30 June 2022

References

- Ju, D. G. *et al.* Clinical significance of tumor-related edema of optic tract affecting visual function in patients with sellar and suprasellar tumors. *World Neurosurg.* **132**, e862–e868. <https://doi.org/10.1016/j.wneu.2019.07.218> (2019).
- Monteiro, M. L., Zambon, B. K. & Cunha, L. P. Predictive factors for the development of visual loss in patients with pituitary macroadenomas and for visual recovery after optic pathway decompression. *Can. J. Ophthalmol.* **45**, 404–408. <https://doi.org/10.3129/i09-276> (2010).
- Wang, H. *et al.* The pattern of visual impairment in patients with pituitary adenoma. *J. Int. Med. Res.* **36**, 1064–1069. <https://doi.org/10.1177/147323000803600525> (2008).
- Yamaguchi, R. *et al.* Sagittal bending of the optic nerve at the entrance from the intracranial to the optic canal and ipsilateral visual acuity in patients with sellar and suprasellar lesions. *J. Neurosurg.* <https://doi.org/10.3171/2019.9.jns191365> (2019).
- Mwanza, J. C. *et al.* Glaucoma diagnostic accuracy of ganglion cell-inner plexiform layer thickness: Comparison with nerve fiber layer and optic nerve head. *Ophthalmology* **119**, 1151–1158. <https://doi.org/10.1016/j.ophtha.2011.12.014> (2012).
- Collette, J., Francois, J. & Neetens, A. Vascularization of the optic pathway. V. Chiasma. *Br. J. Ophthalmol.* **40**, 730–741 (1956).
- van Overbeeke, J. & Sekhar, L. Microanatomy of the blood supply to the optic nerve. *Orbit* **22**, 81–88 (2003).
- Akashi, A. *et al.* The detection of macular analysis by SD-OCT for optic chiasmal compression neuropathy and nasotemporal overlap. *Invest. Ophthalmol. Vis. Sci.* **55**, 4667–4672. <https://doi.org/10.1167/iovs.14-14766> (2014).
- Mortini, P., Losa, M., Barzaghi, R., Boari, N. & Giovanelli, M. Results of transsphenoidal surgery in a large series of patients with pituitary adenoma. *Neurosurgery* **56**, 1222–1233. <https://doi.org/10.1227/01.neu.0000159647.64275.9d> (2005) (Discussion 1233).
- Danesh-Meyer, H. V. *et al.* In vivo retinal nerve fiber layer thickness measured by optical coherence tomography predicts visual recovery after surgery for parasellar tumors. *Invest. Ophthalmol. Vis. Sci.* **49**, 1879–1885. <https://doi.org/10.1167/iovs.07-1127> (2008).
- Moon, C. H., Hwang, S. C., Kim, B. T., Ohn, Y. H. & Park, T. K. Visual prognostic value of optical coherence tomography and photopic negative response in chiasmal compression. *Invest. Ophthalmol. Vis. Sci.* **52**, 8527–8533. <https://doi.org/10.1167/iovs.11-8034> (2011).
- Phal, P. M. *et al.* Assessment of optic pathway structure and function in patients with compression of the optic chiasm: A correlation with optical coherence tomography. *Invest. Ophthalmol. Vis. Sci.* **57**, 3884–3890. <https://doi.org/10.1167/iovs.15-18734> (2016).
- Sun, M., Zhang, Z. Q., Ma, C. Y., Chen, S. H. & Chen, X. J. Predictive factors of visual function recovery after pituitary adenoma resection: A literature review and meta-analysis. *Int. J. Ophthalmol.* **10**, 1742–1750. <https://doi.org/10.18240/ijo.2017.11.17> (2017).
- Yamashita, T. *et al.* Reduced retinal ganglion cell complex thickness in patients with posterior cerebral artery infarction detected using spectral-domain optical coherence tomography. *Jpn. J. Ophthalmol.* **56**, 502–510. <https://doi.org/10.1007/s10384-012-0146-3> (2012).

Acknowledgements

We are grateful to the optometrists of Gunma University for their assistance in acquiring the data used in this study.

Author contributions

The authors were involved in the following aspects of the study: design and conduct (Y.S.); collection of the data (Y.S., R.Y., M.T.); management (Y.S.); analysis (Y.S.); interpretation (Y.S.); preparation of the article (Y.S.); review and final approval of the manuscript (Y.S., D.T., M.T., Y.Y., H.A.).

Competing interests

The authors declare no competing interests.

Additional information

Correspondence and requests for materials should be addressed to Y.S.

Reprints and permissions information is available at www.nature.com/reprints.

Publisher's note Springer Nature remains neutral with regard to jurisdictional claims in published maps and institutional affiliations.



Open Access This article is licensed under a Creative Commons Attribution 4.0 International License, which permits use, sharing, adaptation, distribution and reproduction in any medium or format, as long as you give appropriate credit to the original author(s) and the source, provide a link to the Creative Commons licence, and indicate if changes were made. The images or other third party material in this article are included in the article's Creative Commons licence, unless indicated otherwise in a credit line to the material. If material is not included in the article's Creative Commons licence and your intended use is not permitted by statutory regulation or exceeds the permitted use, you will need to obtain permission directly from the copyright holder. To view a copy of this licence, visit <http://creativecommons.org/licenses/by/4.0/>.

© The Author(s) 2022